NAVAL POSTGRADUATE SCHOOL

MONTEREY, CALIFORNIA

THESIS

ADDITIVE MANUFACTURING OF CONDUCTIVE PARTS USING METAL-POLYMER COMPOSITES

by

Shawn C. Murray

December 2020

Thesis Advisor:	Ibrahim E. Gunduz
Second Reader:	Jonathan Phillips

THIS PAGE INTENTIONALLY LEFT BLANK

REPORT DOCUMENTATION PAGE			*Form Approved OMB No. 0704-0188*

1. AGENCY USE ONLY *(Leave blank)*	**2. REPORT DATE** December 2020	**3. REPORT TYPE AND DATES COVERED** Master's thesis

4. TITLE AND SUBTITLE ADDITIVE MANUFACTURING OF CONDUCTIVE PARTS USING METAL-POLYMER COMPOSITES	**5. FUNDING NUMBERS**
6. AUTHOR(S) Shawn C. Murray	
7. PERFORMING ORGANIZATION NAME(S) AND ADDRESS(ES) Naval Postgraduate School Monterey, CA 93943-5000	**8. PERFORMING ORGANIZATION REPORT NUMBER**
9. SPONSORING / MONITORING AGENCY NAME(S) AND ADDRESS(ES) N/A	**10. SPONSORING / MONITORING AGENCY REPORT NUMBER**

11. SUPPLEMENTARY NOTES The views expressed in this thesis are those of the author and do not reflect the official policy or position of the Department of Defense or the U.S. Government.

12a. DISTRIBUTION / AVAILABILITY STATEMENT Approved for public release. Distribution is unlimited.	**12b. DISTRIBUTION CODE** A

13. ABSTRACT (maximum 200 words)

Additive manufacturing (AM) is used to build a wide array of parts with a unique control of geometry and composition, but it has had limited success in highly electrically conductive three-dimensional (3D) materials. This study investigates the AM of metal-based conductive materials. The research also investigates the mechanical, electrical, and thermal properties of printed parts and printing conditions. The results of the research will help to understand and improve the use of AM of metal-based conductive materials and their applicability to ship board uses. For example, the Navy uses antennas for several applications that require a large amount of surface area and by embedding the antennas in load-bearing bulkheads or other structures, the functional space can be increased.

14. SUBJECT TERMS additive manufacturing, AM, conformal antenna, metal-polymer composite, basic antenna design, conductive polymers, conductive composites, ASTM for metal-polymer composites, antenna theory, mechanical properties of 3D printing, electrical theory of wires, thermal properties of polymer composites, annealing of metal-polymers composites, electrically conductive paste	**15. NUMBER OF PAGES** 69
	16. PRICE CODE

17. SECURITY CLASSIFICATION OF REPORT Unclassified	**18. SECURITY CLASSIFICATION OF THIS PAGE** Unclassified	**19. SECURITY CLASSIFICATION OF ABSTRACT** Unclassified	**20. LIMITATION OF ABSTRACT** UU

NSN 7540-01-280-5500 Standard Form 298 (Rev. 2-89) Prescribed by ANSI Std. 239-18

THIS PAGE INTENTIONALLY LEFT BLANK

Approved for public release. Distribution is unlimited.

ADDITIVE MANUFACTURING OF CONDUCTIVE PARTS USING METAL-POLYMER COMPOSITES

Shawn C. Murray
Lieutenant, United States Navy
BSME, Virginia Polytechnic Institute, 2011

Submitted in partial fulfillment of the
requirements for the degree of

MASTER OF SCIENCE IN MECHANICAL ENGINEERING

from the

NAVAL POSTGRADUATE SCHOOL
December 2020

Approved by: Ibrahim E. Gunduz
Advisor

Jonathan Phillips
Second Reader

Garth V. Hobson
Chair, Department of Mechanical and Aerospace Engineering

THIS PAGE INTENTIONALLY LEFT BLANK

ABSTRACT

Additive manufacturing (AM) is used to build a wide array of parts with a unique control of geometry and composition, but it has had limited success in highly electrically conductive three-dimensional (3D) materials. This study investigates the AM of metal-based conductive materials. The research also investigates the mechanical, electrical, and thermal properties of printed parts and printing conditions. The results of the research will help to understand and improve the use of AM of metal-based conductive materials and their applicability to ship board uses. For example, the Navy uses antennas for several applications that require a large amount of surface area and by embedding the antennas in load-bearing bulkheads or other structures, the functional space can be increased.

THIS PAGE INTENTIONALLY LEFT BLANK

TABLE OF CONTENTS

LIST OF FIGURES

THIS PAGE INTENTIONALLY LEFT BLANK

LIST OF TABLES

THIS PAGE INTENTIONALLY LEFT BLANK

LIST OF ACRONYMS AND ABBREVIATIONS

3D	Three-Dimensional
°C	Degrees Celsius
AM	Additive Manufacturing
ANSI	American National Standards Institute
ASTM	American Society for Testing and Materials
CAS	Chemical Abstracts Service
cm	Centimeter
HDTV	High-definition Television
IACS	International Annealed Copper Standard
mm	Millimeter
MPa	Mega Pascal
PLA	Polylactic Acid
RPM	Revolutions per Minute
SEM	Scanning Electron Microscope
UV	Ultraviolet
µm	Micrometer
USB	Universal Serial Bus

THIS PAGE INTENTIONALLY LEFT BLANK

EXECUTIVE SUMMARY

This study was performed to expand the knowledge and understanding of the additive manufacturing (AM) of conductive metallic materials in a metal-polymer composite matrix. Additionally, the study was conducted to explore the application of AM of antennas used by the U.S. Navy. The study started with aluminum, copper, tin, and titanium metal powder candidates in addition to three polymer candidates: polyvinyl, polyamine, and ultraviolet (UV) cured epoxy. After characterization of the metal powders and polymers, the study downselected to two metal powders: copper (Cu-110) and titanium Ti-64), and one polymer, polyamine in a two-part epoxy form.

Next, the study used solution casting to create cylinder-shaped composites of ten various diameters, ranging from 14 gauge to 30 gauge, and nine different weight fractions, ranging from 86–94% by weight. The study measured the resistivity of the samples, and found titanium samples had consistent measurements across all diameters. This led to the conclusion that the thickness of the conductive layer for titanium is less than 30 gauge or a layer thickness of 0.16 mm. However, the study found an open-circuit reading for all copper samples, which was not expected and resulted in the study downselecting to use only titanium for the next stage of the experiment. In addition, the study found titanium with epoxy volume fraction of 70% to be the efficient mixture to proceed into modeling.

Next, the study 3D-printed models of various antennas, ranging from high-definition television (HDTV) to Wi-Fi signals, to conduct a go/no-go test of the Ti-64 composite material and black polylactic acid (PLA) filament. The study found Ti-64 composite material and black PLA is a low-cost option for antenna applications in the HDTV and 2.4 GHz Wi-Fi range. Ultimately, the study continued to expand the understanding and use of AM applications for the U.S. Navy.

THIS PAGE INTENTIONALLY LEFT BLANK

ACKNOWLEDGMENTS

I would like to thank my family for their love. You will never get the time back lost from my late night studying, research, and extensive work hours I committed to this process, and I appreciate your understanding and support throughout it.

I would like to thank my thesis advisor, Professor Ibrahim E. Gunduz, for his guidance, teaching, and assistance with this study.

In addition, I would like to thank Professor Jonathan Phillips as my second reader for his support in this study.

Likewise, I would like to thank Professor Dragoslav Grbovic and Professor Troy Ansell for their aid with the SEM; both made great efforts to assist me and other students at NPS.

Furthermore, I would like to thank PO1 Andrew Reagan, USN, from the Robo Dojo for assistance in 3D printing.

In addition, I would like to thank Rebecca Pieken from TPO for her aid in creating this document. Thank you for answering all of my questions.

THIS PAGE INTENTIONALLY LEFT BLANK

I. INTRODUCTION

A. MOTIVATION

Additive manufacturing (AM) covers the building of a wide array of building parts and tools, including electrically conductive three-dimensional (3D) materials. Shipboard applications of these materials could be conformal antennas and electrical components that are embedded in load-bearing structures providing strength and other functions like enhanced thermal conductivity. In terms of performance, structures can be built using AM methods through strict control of component geometry. However, scalable applications of these materials through AM methods are not conducted due to the limited materials accessible for manufacturing. These limited materials typically have poor electrical performance or require large costs to achieve electrical performance goals.

The study investigates AM of low-cost metal-based heterogeneous composite materials that are known to be electrically conductive. Specifically, the composition of the materials was varied with different mass fractions of metal powders, such as aluminum, copper, tin, and titanium mixed with polymer binders. Additionally, commercially available conductive filaments was used for printing. The electrical properties of the printed paths were measured. Once optimum processes and material settings are determined to yield the best performance parameters, more complex shapes are printed, such as high-definition television (HDTV) and Wi-Fi antennas. Lastly, the antennas and other structures are evaluated for applicability throughout Navy vessels. For example, the Navy uses antennas for several applications, which require a large surface area. By embedding the antennas in load-bearing bulkheads or other structures, the vessel could have more functional space available.

This study would contribute to the ability to fabricate complex design multifunctional parts, such as structural antennas and can help gain valuable surface space on board vessels. In addition, the study works to advance electrically conductive 3D materials built through the AM processes. The 3D antennas can have a much wider broadband response, compared to two-dimensional antennas. The success of this study could lead to reducing the radar cross

section of the vessel by reducing externally attached communication equipment. By reducing the number of external attachments, a secondary effect would be reducing the visual signature of the vessel.

B. BACKGROUND

1. AM Brief History and U.S. Navy Application

In [1], Kocovic demonstrated how Hideo Kodama developed a new system that would change the world [1]. In 1981, Kodama built a system for rapid prototyping that used photopolymer, which initiated an AM blitz [1]. In 1983 and 1986, several breakthroughs were accomplished with this new technology, but the true advancement came in 1988 when Scott Crump created the system that is still used today [1]. A layer-by-layer system known as fused deposition modeling helped to drive the next three decades of advancement and development in AM technology [1]. As AM technology continued to develop it expanded into various other areas, which included the biomaterial industry, the medical industry, the dental industry, the automotive industry, the food industry, the aircraft industry, the space industry, and the robotic industry. Among all of this expansion, one of the most significant expansions was the application of AM technology to the military [1], [2]. In [2], the study examined the benefits and drawbacks to AM technology in the military [2]. When addressing possible future applications of AM technology for different service branches, the study used the Navy and a scenario where a F-35C aircraft stereo needed a part, created by AM technology onboard a navy vessel underway [2]. This stereo expands not only to aircrafts, but also to ships, submarines, navy vehicles, and other vessels [2]. Both [1] and [2] agree there are benefits and drawbacks to AM technology. The benefits addressed are increased flexibility of manufacturing, decreased part expenses, decreased manufacturing time, increased prototyping, increased use of complex geometry, and decreased storage use for parts [1], [2]. The two main drawbacks outlined by [1] and [2] were limited materials that can be used by 3D printing machines and copyright complications with AM technology used to reproduce a manufactured item. However, the benefits of AM technology make it an essential asset for current and future uses in the U.S. Navy.

2. Electrical Conductivity of Metal Powders

From [3], Electrical behavior of oxidized metal powders during and after compaction found tantalum and aluminum pure unoxidized powders had a reduction in resistivity of >10^6 ohm-cm over a compaction stress range of 1 MPa to 10 MPa [3]. The study found that as the stress increased the electrical field decreased for the powder sample [3]. Other studies looked at copper, nickel, copper-nickel mixtures, and iron for investigating electrical behavior of metal powders [3]. As pressure increased, copper powder conductivity had steep increases [3]. As pressure for the copper was increased from two MPa to five MPa the conductivity of the forty angstroms powder increased by an order of seven [3]. The study found that compacted tantalum and aluminum powder resistivity followed similar trends to that of copper. The study used Hertzian equations to calculate the contact area of two particles [3]. In addition, the study found that breaks in the oxidized layer did not affect resistivity until metal-to-metal contact occurred [3].

In [4], Montes, Cuevas, and Cintas looked at the application of an equation to predict the resistivity of oxidized compressed metal powders. The equation considered the sintering conducted by electrical current and analyzed the aluminum, bronze, iron, and nickel metal powders that were compressed [4]. The equation is consistent with the percolation theories [4]. The study considered the effect of porosity of the packed sample, and found descaling and particle shape effects the formation of electrical paths in the sample [4]. Likewise, the study found it difficult to accurately predict the thickness and resistivity of the oxidized layer [4]. The study documented success with the theoretical and experimental values supporting one another [4].

In [5] expanding the work of [4], the study considered conductivity and how it reacted to the oxidized layer of thickness and porosity. The study's equation aligns with percolation theory [5]. The study examined aluminum, bronze, iron, and nickel metal powders under various compression pressures and found as porosity decreases conductivity increases [5]. The study noted that the particle size, particle shape, and particle distribution effect its conductivity [5]. The study conducted electrical measurements during compression; however, the measurements did not take into account elastic recovery of the oxidation film between metal particles [5].

3. Electrical Conductors

According to [6], electrical discharge machining is heavily effected by electrode performance. This technique requires minimum to no defect of the electrode [6]. In addition, this technique causes erosion of materials immersed in a dielectric solution [6]. Many factors affect the interaction between the material and the electrode, which ultimately affect the properties of the sample [6]. The study stated that as compacting pressure increased, performance increased [6].

In [7], the study analyzed the effects of particle size, pressure, electrical field strength, field frequency, rate at which pressure was applied, and type of compression on metal powders' conductivity. The study examined metal powder used in batteries, which ranged from manganese dioxide, graphite, carbon black, black mix, nickel, and lead oxide [7]. The study found metal powder conductivity increased as pressure increased, until conductivity became constant after reducing the number of voids [7]. Furthermore, the study found conductivity decreased as rate at which pressure was applied increased [7]. However, the study was unable to determine a number of the effects due to the complex nature of the materials [7].

4. 3D-Printed Electrical Wires

In [8], the study examined a copper core with a silver-coated shell nanowire used in 3D printing. The study concentrated on large aspect ratios to create a polymer composite with high electrical conductivity [8]. In addition, the study focused on nanowires for 3D printable inks at low volume fractions [8]. The study found the resistivity of the nanowire to be 0.002 ohm-cm [8]. The study exposed the nanowire to an environment of eight-five degrees Celsius and a relative humidity of 85% for twenty-four hours to determine the thickness of the silver shell needed to maintain conductivity [8]. The study found a critical volume fraction of the nanowire filler in the composite where the resistivity no longer decreased and became constant [8]. The study determined a 12% by volume loading of the nanowire was optimal to create a conductive composite after extrusion in the 3D printing process [8]. In addition, the study found surface roughness of the composite increased as weight percentage of the nanowire increased, which caused decreased conductivity [8].

5. Conductive Polymers

In [9], Araujo and Rosenberg studied the conductivity of aluminum, bronze, copper, gold, lead, silver, stainless steel, and tin mixed into an Epikote 828 resin. The study based the experiments on two different theories, one of which was proposed by Maxwell and Rayleigh, and was later built upon by Meredith and Tobias [9]. This theory states that particles form an array inside of an insulating matrix, but never comes in contact with another particle [9]. The second proposed theory states a number of particles in a random array will form a conducting path due to metal-to-metal contact of the particles [9]. This is known as the percolation theory, proposed by Scher and Zallen, and later expanded on by Seager and Pike [9]. The study looked at spherical particles with a mean diameter less than one hundred μm and in volume percentages at 10, 20, 30, 40, and 55 particle loading [9]. The samples in the study were cured by cooling at 125 °C for sixteen hours or 200 °C for four hours [9]. The samples cooled for four hours were found to be non-conductive due to the resin undergoing thermal expansion [9].

In [10], the study compared silver-coated copper particles from electro plating in a polymeric resin against copper particles in a polymeric resin. The study selected silver coating mainly to overcome copper oxidation [10]. The study determined that the metal drives the adhesives electrical properties and thermal properties, where the resin drives the mechanical properties [10]. The study noted the increases in cost to manufacture silver adhesives [10]. The study examined different silver to copper mass ratio of zero, five, and ten, and two different shapes, spinous and spherical [10]. Forty samples were tested and the sliver coated copper particles in a polymeric resin had lower resistivity and reduced oxidation, than those of pure copper particles [10].

In [11], the study created a stretchable conductive polymer, and implemented strain engineering and nanocomposites as two methods for manufacturing the desired conductor [11]. The study examined ionic liquids due to the availability of the material [11]. The study considered an elastic substrate and its effects on conductivity [11]. The study examined how temperature dependence was effected by composition and morphology of the sample and the relationship to conductivity [11]. After one hundred cycles at one hundred percent strain, the study found the conductivity of the sample to hold at 3600 S/cm [11].

6. Solution Casting

From [12], electrical conductivity of Cu-powder dispersed in a PMMA composite was prepared by solution-cast, found as the Cu-powder particle size increased, the distribution increased until 30% where the distribution plateaued. The distribution plateaued collated to a Cu-powder particle size between 50 μm to 100 μm [12]. One AM method is solution casting, starting with a metal powder, a resin and a catalyst are mixed together, and the mixture is poured into a mold and pressed until cured, as shown in Figure 1 [12]. Ebihara and the team found that as volume percentage of Cu-powder increases, the effect of voltage on current density increases linearly [12]. In addition, resistivity has an exponential decrease as volume fraction of copper increases in bulk sample on a log scale [12]. The trend leveled off between 40% to 50%. Lastly, the study found that the Cu-powder dispersed in PMMA composite had a critical point for conductivity, where increases in volume fraction of the Cu-powder did not increase the conductivity of the composite [12].

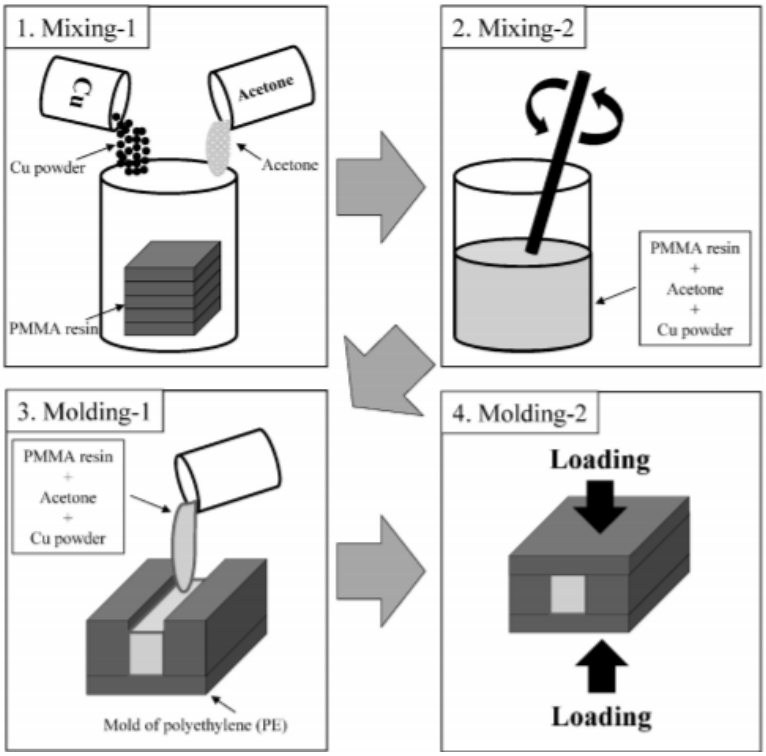

Figure 1. Steps for solution casting. PMMA polymer, copper powder, and acetone were used. Source: [12].

7. Conductive Composites

In [13], the study examined copper-polymer composites conductivity; as well as, stated that conductive plastics are inexpensive, lightweight, and have a high manufacturability [13]. The study addressed percolation theory, where conductive paths shift from inhomogeneous to homogeneous in the polymer matrix, driven by contact of the metal particles in the matrix [13]. The study supports the effect on conductivity from uniform shape of particles in the composite [13]. The study found the use of hydrogen and nitric or hydrochloric acid is the most effective method to prepare copper powders for use in samples [13]. The study recommended cleaning copper materials sourced from commercial sellers [13]. The study used synchronous detection and direct measurement of dc voltage for each samples for resistivity [13]. The study referenced Hertz, Sharvin, and Maxwell equations to model the sample in different ways [13]. In addition, the study provided recommends for future creations of metal polymer matrixes, which were to verify the metal powder is clean before use, minimize heat input, minimize oxidation, use solvents that evaporate, and use particles shaped to maximize metal-to-metal contact [13]. Furthermore, the study analyzed electrical noise in the composite [13]. The study found the electrical noise was effected by resistance, temperature, current, and frequency [13]. The study found noise was dependent on the space between metal particles in the composite [13].

According to Alan Lyons in [14], epoxy matrixes with either silver-plated glass particles or sliver-plated nickel particles, with small particle sizes of thirty-seven μm to forty-four μm and large particle sizes of less than forty-four μm distributions, found that small particle size distributions needed higher particle loading to cause a steep decrease in the electrical resistivity, also known as the percolation threshold [14]. The study also found that the amount of particle loading needed to reach the percolation threshold was directly affected by the processing methods [14]. In addition, the study looked a low aspect ratio, and used two different types of spherical particles to create the smallest surface area to volume [14]. Laser light scattering was then implemented to analyze the distributions of particles [14].

In [15], the study looked at copper and aluminum metal-filled composites using solvent casting technique. The study worked to create conductive polymer by two methods [15]. The first method used a small number of doping agent macromolecules and the second method used metal filler in a poly resin [15]. This study focused on the second method [15]. The study relied on the percolation theory to describe the interactions between particles based on geometry and quantity of particles [15]. The study predicted at 20% by volume of metal filler the sample would see a decrease in resistivity by 10^{10} ohm-cm [15]. The study examined thirty-nine specimens, which consisted of copper or aluminum fillers [15]. The study observed a switching event and found that as temperature increased, the threshold decreased [15].

8. Annealing of Metal-Polymer Composites

In [16], the study examined properties of aluminum epoxy composites against aluminum/nickel epoxy composites in order to take advantage of reduced weight, oxidation, complexity in manufacturing, and expenses. The study used positron annihilation lifetime spectroscopy to examine voids in the material samples [16]. The study used a two-part epoxy and placed it under a vacuum to remove air pockets [16]. The study noted several trends, including reduced strength, reduced hardness, and increased conductivity as aluminum concentration rose to 30% by weight [14]. It was also noted that as the nickel concentration increased it caused strength to be reduced and hardness to be increased [16]. In addition, the study found that as electron density increased, annihilation lifetime decreased, and that the highest conductivity was reached at an aluminum percent by weight of forty [16].

9. Mechanical Properties of 3D Printed Composites

In [17], SEM was used to examine aluminum, tin, and zinc powders loaded into an epoxy resin composite at the matrix interface. The study analyzed the conductive behavior of the composites and found it to be nonlinear [17]. The study examined the structural, thermal, and electrical properties of the composites, and their morphology, which were found to be random with a homogeneous morphology [17]. The study determined the composites to be a binary system with voids and pores through the composite [17]. The

study described as percentage weight of the metal powder was increased, the composite density increased [17]. In addition, the study found porosity decreased as metal filler increased [17]. Furthermore, the study documented that the crystal lattice peaks increased as percentage weight of metal powder was increased [17]. The study found the conductivity of the composited followed percolate theory and the critical value was determined to be at 15% by volume [17]. The results explained that conductivity was dependent on porosity, particle shape, particle size, resin viscosity, surface tension, and surface energy [17].

10. Thermal Properties of Polymer Composites

In [18], aluminum particles imbedded in a poly(methyl methacrylate) were examined for a critical value, which was indicated by a steep drop in resistivity. The study found the critical point to be between 20% to 30% by volume of metal filler, consistent with other studies [18]. The study explained an electrical field could be applied as low as twenty-five volts per centimeter to reach the critical value [18]. The study identified the presence of carbonaceous particles when the sample reached the critical value [18]. In addition, this state was found to be irreversible at twenty-five degrees Celsius, but could be reversed at one hundred and four degrees Celsius for ten minutes [18]. The study found thermal breakdown of the metal polymer composite occurred at megavolts per centimeter with the formation of cracks propagating conductive paths [18]. The study also recognized the percent volume of the metal filler needed for thermal breakdown to occur was linked to the shape of the metal particles and how the material was prepared [18].

In [19], metal epoxy composites were examined with the use of the percolation theory. The study looked at aluminum, copper, and zinc metal powders at various temperatures, ranging from twenty degrees Celsius to one hundred forty degrees Celsius [19]. The study looked at a critical concentration where the composite becomes conductive and electrical current flows through the composite [19]. As the concentration of the metal powder in the composite increased, the conductivity increased until the critical concentration was reached [19]. In addition, the study found that as temperature increased the conductivity also increased [19]. Likewise, the study found that percolation theory was

not effected by temperature, and as the metal powder particle size was increased, a reduction in the critical concentration was observed [19].

11. AM of Conductive Metallic Materials Using External Fields

In [20], Kwan, Shin, and Tsui found that electrical current follows discrete paths in composites of mixed Polylite 499 and MEKP resin with silver powder particles spheres or silver coated glass particle spheres. The study found the samples to displace voltage switching and were non-ohmic [20]. The study identified silver powder particles spheres with a particle size of approximately one μm achieved the threshold voltage with a volume concentration from zero to 6% [20]. Additionally, the study found silver-coated glass particle spheres with a particle diameter of approximately ten μm achieved the threshold voltage with a volume concentration from 0% to 30% [20]. The samples were prepared by mixing the Polylite 499 and MEKP together, and then mixing the silver powder particles spheres or silver-coated glass particle spheres into the mixture [20]. The mixture was degassed and placed on a rotor at five rev per min in an oven set at sixty degrees Celsius for sixteen hours [20]. The sample was then polished and a silver epoxy was added to all sides, and then cured again at sixty degrees Celsius for two hours [20]. The study proposed the electron hopping occurred to reach the threshold voltage and then metallic filament occurred once the flow of current was established [20]. This occurrence has been noted in other studies using copper oxide as well [20].

12. Electrically Conductive Paste

In [21] the study examined silver-aluminum nanopaste at different weight percentages of aluminum and sintered the samples at three hundred eighty degrees Celsius for thirty minutes [21]. After which the study examined thermal and electrical conductivity, and looked at die-attached nanoscale material and their application to manufacturing lines [21]. The study conducted weight percent in steps of twenty from zero to one hundred [21]. In addition, the study used a pressure of 10.34 MPa to maintain the samples before sintering [21]. The study found porosity increased and density decreased; in addition, the use of large size particles minimized shrinkage after sintering [21]. The study found conductivity decreased as percentage weight of aluminum increased, the study attributed this to the

increased oxidation of aluminum [21]. Also, it was noted that porosity increased, thermal conductivity decreased, and thermal diffusivity decreased as percent weight of aluminum increased [21].

13. AM Effects on Attenuation of Electromagnetic Waves

In [22], the study examined aluminum metal flakes in an epoxy composite with electrical properties. The study found insertion loss was influenced by frequency and that effect was increased as the metal filler was increased [22]. The study's results supported other studies conducted with nickel coated carbon particles in a composite [22]. The study found characteristics of the filler greatly affected electromagnetic wave attenuation [22]. In addition, the study found shielding effectiveness increased as metal filler increased or thickness increased [22]. The study determined the critical point for the aluminum filler to be between 5% to 10% by weight [22].

C. OBJECTIVES

This research investigate the AM of heterogeneous materials, including metal-polymer mixtures. The specific research questions are; 1. How does the powder content affect the electrical conductivity of the materials of interest? 2. How do the prepared and printed materials of interest perform as antennas?

D. ASSUMPTIONS AND LIMITATIONS

The study was limited due to the hindrance of the COVID-19 pandemic on acquiring materials and equipment to conduct the study; including, delayed access to the labs and equipment to conduct the experiments.

THIS PAGE INTENTIONALLY LEFT BLANK

II. EXPERIMENT

A. MATERIAL SELECTION

1. Metal Selection

The experiment work began with identifying metal powder candidates with the highest electrical conductivity for use. The selected metal powders were aluminum, copper, tin, and titanium. Three different powder sizes were used for copper. Together these powders provided six material candidates, as shown in Table 1, to use in the experiment with the expected conductivity, resistances, and %ICAS as shown in Table 2 for the selected powders [23].

Table 1. Metal powder candidates material data

Powder Type	Acronym	Powder Size	Batch Number	Lot Number	CAS Number	Manufacturer
Aluminum	Al-101	99% -325 mesh	A	1805521	7429-90-5	Atlantic Equipment Engineers
Copper	Cu-115	99.9% -100 mesh	AINJQ00001	1710507	7440-50-8	Atlantic Equipment Engineers
Copper	Cu-112	99.9% -325 mesh	AINJQ00001	1807504	7440-50-8	Atlantic Equipment Engineers
Copper	Cu-110	99.9% 1-5 micron	AINJQ00001	1809505	7440-50-8	Atlantic Equipment Engineers
Tin	Sn-102	99.9% -325 mesh	AINJQ00001	1806500	7440-31-5	Atlantic Equipment Engineers
Titanium	Ti-64	Not Given	A	U281701	Not Given	EOS Emanufacturing Solutions

Table 2. Resistance, conductivity, and percent IACS of pure metals. Source: [23].

Pure metal	Resistance (ohm-m)	Conductivity (Siemens/m)	% IACS
Aluminum	2.826E-08	3.54E+07	61
Copper	1.724E-08	5.80E+07	100
Tin	1.149E-07	8.70E+06	15
Titanium (Ti-64)	1.724E-06	5.800E+05	1.0

Each powder was examined by an Inspect F50 SEM, manufactured by FEI company. The SEM micrographs were taken at 5 KeV and a working distance between 11.2 mm and 11.8 mm. Three areas were analyzed at 100x, 500x, and 1000x magnification.

After a review of the powders, the study downselected from six to two metal powders with uniform round shapes. The copper spherical powder (Cu-110) and titanium (Ti-64) powder were selected for the mixtures, using copper (Cu-110) as a baseline to compare titanium (Ti-64) against.

Next, the two powders were placed in a Partica laser-scattering particle size distribution analyzer LA-95OV2 built by Horiba. The powder was placed into a dry feeder on top of the machine with the machine feeder speed set to 34 automatic, with a transmittance (R) upper limit set at 100 % and a lower limit set at 95%. The data acquisition times (sample) were set at 20,000 and the data acquisition times (blank) were set at 5,000. The Stop trigger was set at T% 99.5.

2. Polymer Selection

For the experiment, three different polymer candidates were selected. The first was Mowital B 30HH Kuraray Polyvinyl Butyral (lot number DE10023530 manufactured by Kuraray America Inc.) dissolved in ethanol. The second was a two part epoxy 20–3237CCL16 polyamine formulation (lot number BT111287 manufactured by Epoxies Inc.) with 20–3237RCL15 epoxy resin formulation (lot number BT109911 manufactured by Epoxies Inc.). The third was 607105RCL13 UV Formulation (lot number BT110451 manufactured by Epoxies Inc.)

B. SAMPLE PREPARATION

Metal powders were weighed on a digital balance (model USS-DBS8 manufactured by U.S. Solid Laboratory Equipment) and polymers were mixed before added to the metal powders in small batch samples ranging from 86% - 94% by weight. For example, the polyvinyl butyral-ethanol mixture and the two-part epoxy, the polymers were weighed and manually mixed before the metals powders were added. An example of this would be the two-part epoxy and catalyst, which was mixed at a 1:1 ratio, thus equal parts of polyamine

and resin were manually mixed. The combined epoxy was then added to the metal powder to achieve the desired overall weight ratio. The samples were manually mixed, taken to a vacuum, and then mixed in a Speed Mixer DAC150.1 FVZ-K (serial number 1057A17503 manufactured by Hauschild Germany). The samples were approximately 5g in total mass.

The samples were initially mixed for two minutes at 3000 revolutions per minute (RPM), and then reduced to 1200 RPM for two minutes. The goal was to obtain a sample with play-dough like consistency that would hold its shape after deposition; however, the samples heated and poor mixing occurred. The effects of heat on the mixture was not investigated in this study, but was minimized to prevent sample curing. The study found adequate mixing and minimum heat input by mixing at 1200 RPM for one minute. Some of the material that was near the bottom corners of the container were scooped to improve mixing. The sample was then mixed for ten seconds at 3000 RPM, after which the corners were scooped again. This process was repeated three times. As seen in Figure 2, the final material had a smooth plastic consistency.

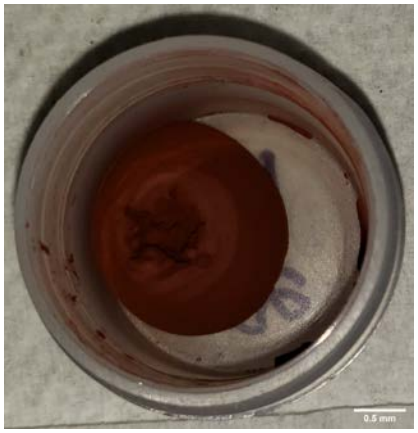

Figure 2. Copper (Cu-110) mixed with two part epoxy at 93% by weight

Next, the sample was placed in syringes and extruded through different sized nozzles. Due to resource limitations, four different sized diameter 3D printed nozzles initially were used, as seen in Figure 3.

Figure 3. 3D printed nozzles

The study had initial success with 3D printed nozzles with varying sized holes, as seen in Table 3. However, extrusion was found to be inconsistent at fine sizes and at increased solids loading. The study transferred to Brostown 13.7 mm industrial blunt tips. As documented in Table 4, the needles ranged from 14 gauge to 30 gauge [24].

Table 3. 3D printed nozzles versus weight fraction

Cu-110 Weight Fraction Wanted (%)	Nozzle 1 Extrusion	Nozzle 2 Extrusion	Nozzle 3 Extrusion	Nozzle 4 Extrusion
90	Successful	Successful	Successful	Successful
91	Successful	Successful	Unsuccessful	Unsuccessful
92	Successful	Successful	Unsuccessful	Unsuccessful
93	Unsuccessful	Unsuccessful	Unsuccessful	Unsuccessful
94	Unsuccessful	Unsuccessful	Unsuccessful	Unsuccessful

Table 4. Needle data for different gauge size. Source: [24].

Gauge size	Inner Diameter(mm)	Outer Diameter (mm)	Color
14	1.55	2.1	Olive
15	1.36	1.8	Amber
18	0.84	1.27	Green
20	0.6	0.92	Pink
21	0.51	0.82	Purple
22	0.41	0.72	Blue
23	0.34	0.64	Orange
25	0.26	0.52	Red
27	0.21	0.42	Clear
30	0.16	0.31	Lavender

Next, the samples were extrude on glass slides, as seen in Figure 4. The lengths of the lines ware measured. In addition, the study used 689.476 KPa low pressurized air to extrude the material from the syringes using an air compressor (SN1315106U3520010 manufactured by Husky) and a universal syringe adapter (model number 5VZW1 manufactured by Weller). In early batches, the material was inconsistently deposited on the glass slides. The resistance was measured on a multimeter (Fluke 110), the copper samples showed an open circuit condition. This was not expected since the copper material formed conductive traces in the initial trials. The samples were redone with a modification, Chipquick SMDIN52SN48 In 52/Sn 48 Solder with SMD291 Flux used to create a better measurement point at each end of the samples, as seen in Figure 5. The copper samples showed an open circuit condition again. The process was repeated at different weight fractions, and copper repeatedly measured as an open circuit. The mostly likely cause of this reading was due to air exposure of the fine copper particles allowing the formation of oxides and hydrides to cover the surface of the particles.

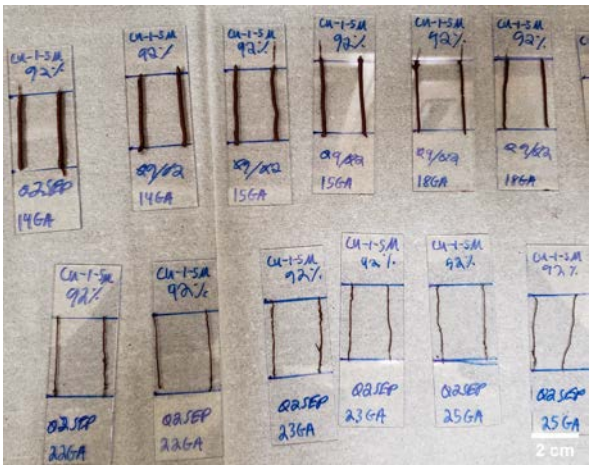

Figure 4. Copper (Cu-110) epoxy composites on glass slides

Figure 5. Copper (Cu-110) epoxy composites on glass slide with solder ends

The study refined the process for solution casting and added copper tape to provide the contacts on each end of the sample. As opposed to copper samples, titanium based samples provided consistent results with low resistance. The resistance of titanium with 70% percent by volume in a two-part epoxy composite, as seen in Figure 6, was found to be constant across a range of gauge sizes, as shown in Table 5. The conductive layer thickness for titanium has an upper bound of 0.16 mm, but possibly less when compared with the average particle size of ≈ 0.03 mm.

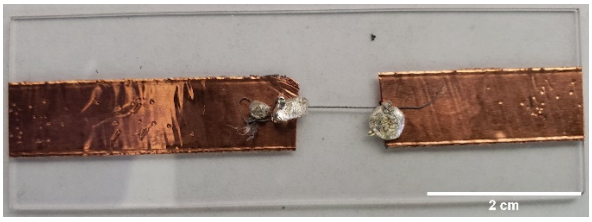

Figure 6. Titanium (Ti-64) epoxy composites on glass slide with solder and copper tape at ends

Table 5. Titanium and two-part epoxy composite resistance measurement at different gauge sizes.

Gauge	Percent by volume	Percent by weight	Measurement 1 Resistance (ohm)	Measurement 2 Resistance (ohm)	Measurement 3 Resistance (ohm)
14	70	90	31.3	31.3	31.3
22	70	90	26.3	26.3	26.3
30	70	90	33.0	33.0	33.0

C. ANTENNA PREPARATION

Next, the study built three different antennas to test the titanium and two-part epoxy polymer mixture and 1.75mm black Polylactic (PLA) filament (190520, manufactured by Proto-pasta). First, a SOLIDWORKS model was created for each antenna based on designs from [25] for a HDTV antenna, as seen in Figure 7, [26] a Wi-Fi antenna, as seen in Figure 8, and a Wi-Fi antenna from a 2.4 Linksys wireless B universal serial bus (USB) network adapter 802.11b from Cisco systems, as seen in Figure 9.

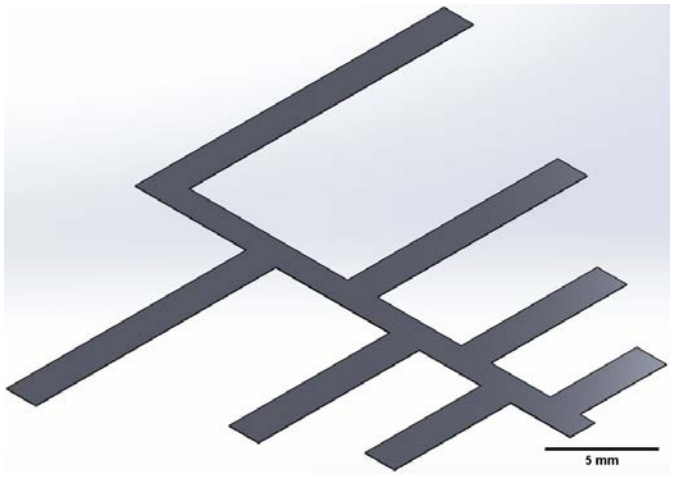

Figure 7. SOLIDWORKS model of the HDTV antenna

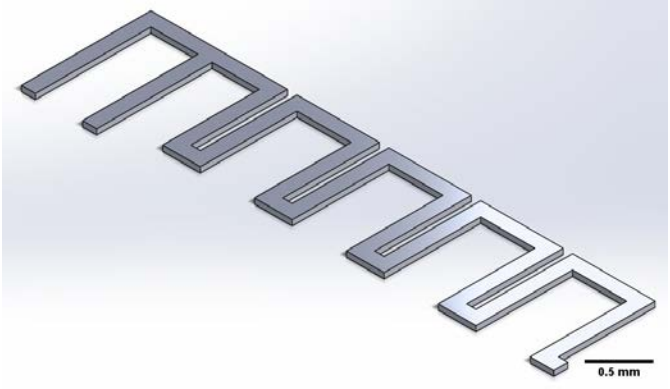

Figure 8. SOLIDWORKS model of the Wi-Fi antenna

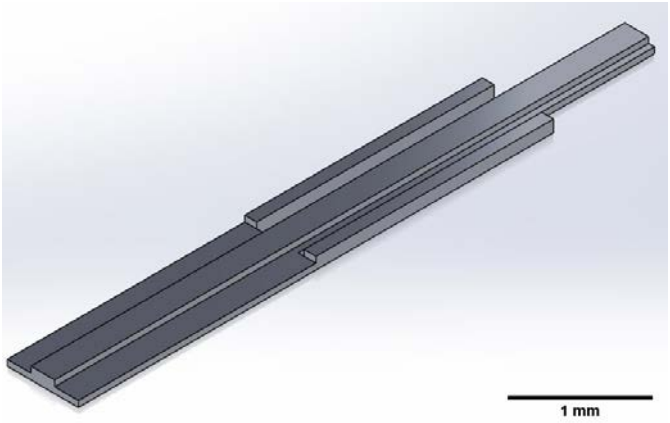

Figure 9. SOLIDWORKS model of the Linksys antenna

Next, the designs were loaded into Cura 15.04.6 slicing software manufactured by Uitimaker and printed with a MP Mini Delta / Malyan M300 3D printer manufactured by Monoprice. Copper tape was attached to the printer antennas and a wire was soldered with lead solder.

Next, the models were subtracted out of a block, as seen in Figures 10, 11, and 12. The models were loaded into Cura 15.04.6 slicing software. The slicing software converted the SOLIDWORKS model into a G-code or machine code for the 3D printer to use. The G-code provided x, y, and z coordinates to print each antenna. The HDTV antenna was printed on a Ultimaker S5 Pro 3D printer (manufactured by Ultimaker) and the two Wi-Fi antennas were printed on a MP Mini Delta 3D printer (manufactured by Monoprice). This was done to

meet the required size of the HDTV antenna. The 70% volume fraction of titanium and two-part epoxy polymer mixture were then pressed into the 3D printed molds by hand. Copper tape was attached to the printer antennas and a wire was soldered with lead solder.

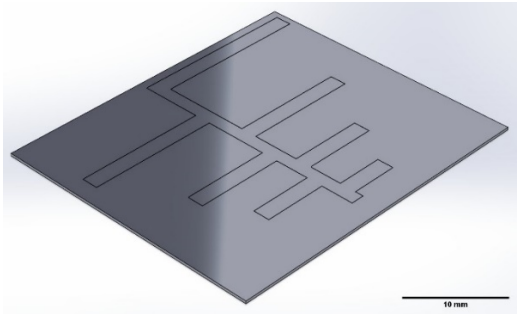

Figure 10. SOLIDWORKS model of a HDTV antenna subtracted from a block

Figure 11. SOLIDWORKS model of a Wi-Fi antenna subtracted from a block

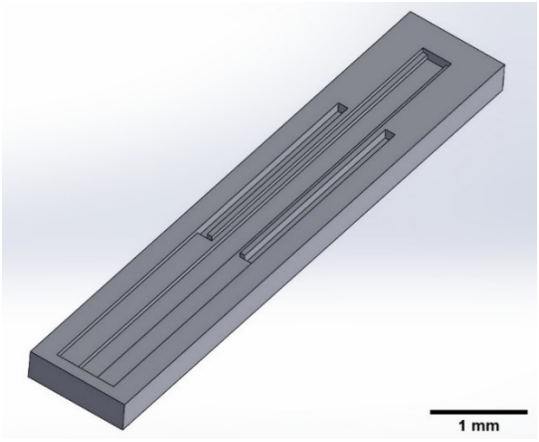

Figure 12. SOLIDWORKS model of a Linksys antenna subtracted from a block

D. ANTENNA TESTING

The antennas were tested by connecting the HDTV antennas one at time to a TV (manufactured by Insignia) and the Wi-Fi antennas were connected in a set of two to a 2.4G Wi-Fi repeater (N 300M manufactured by Tentsky). The TV test was baselined with no antenna attached and the results are in Table 6.

Table 6. HDTV antenna test results

Antenna type	Number of analog channels found	Number of digital channels found	Average signal strength
None	0	0	0
Ti-64 antenna	1	10	58%
Black PLA	0	20	55%

The Wi-Fi antenna baseline was conducted with the original antennas that were attached to the Wi-Fi repeater and with wires that were the same length at 38.5 mm, as see in Figure 13 and Figure 14. The signal strength was recorded in Table 7.

Figure 13. Original Tentsky Wi-Fi antenna

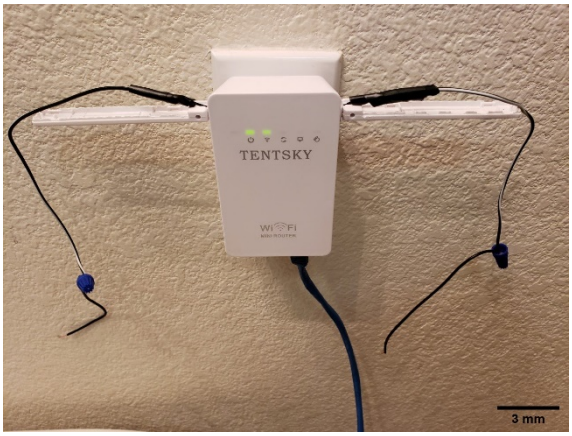

Figure 14. Test setup for Wi-Fi antennas with wire baseline

Table 7. Wi-Fi antenna signal strength test results

Antenna design	Minimum signal strength (dB)	Maximum signal strength (dB)
Original Tentsky	-26	-23
wire only	-58	-51
Ti-64 Wi-Fi	-46	-42
Black PLA Wi-Fi	-54	-43
Ti-64 Linksys	-49	-41
Black PLA Linksys	-39	-36

THIS PAGE INTENTIONALLY LEFT BLANK

III. RESULTS AND DISCUSSION

A. SEM MICROGRAPHS

As seen in Figures 15–20, Al-101, Cu-115, Cu-112, and Sn-102 were found to be non-spherical. Figures 27–38 shows SEM micrographs for are two and are three for all six metal powders.

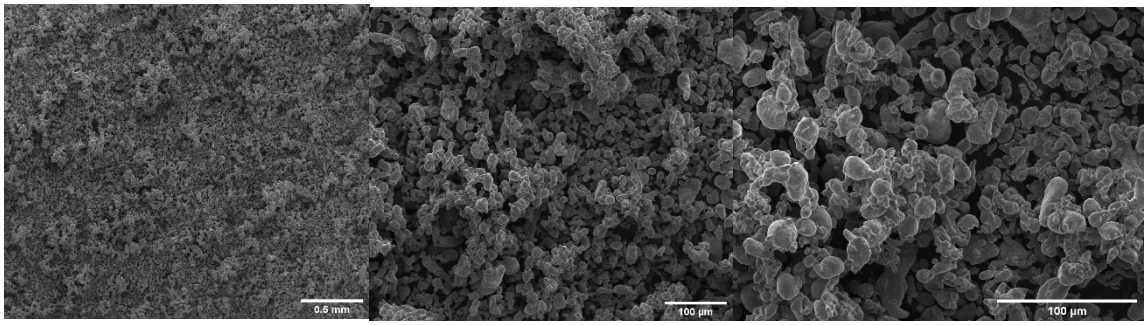

Figure 15. Area one. Aluminum (Al-101) powder size at -325 mesh. Left 100x magnification; middle 500x magnification; right 1000x magnification

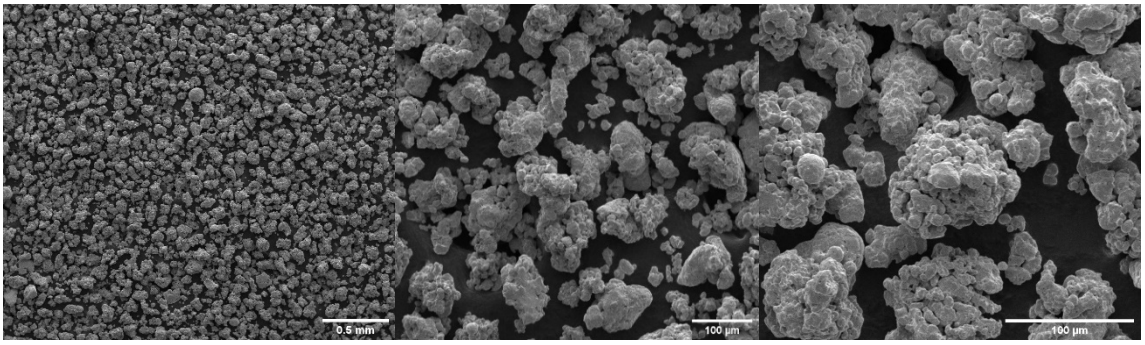

Figure 16. Area one. Copper (Cu-115) powder size at -100 mesh. Left 100x magnification; middle 500x magnification; right 1000x magnification

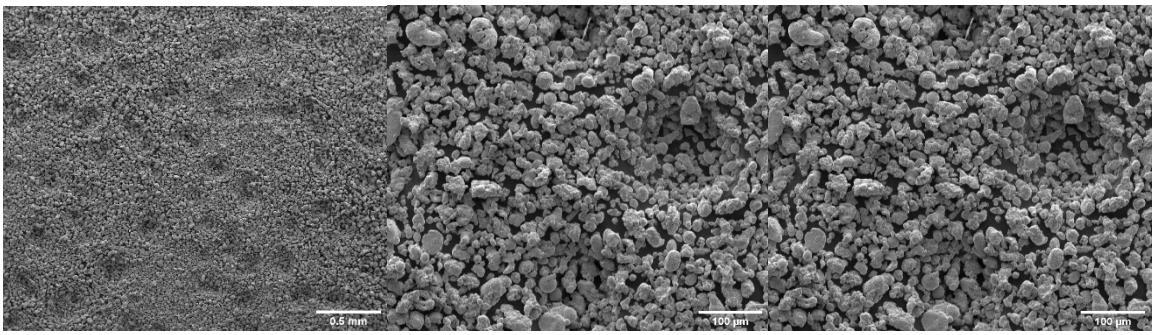

Figure 17. Area one. Copper (Cu-112) powder size at -325 mesh. Left 100x magnification; middle 500x magnification; right 1000x magnification

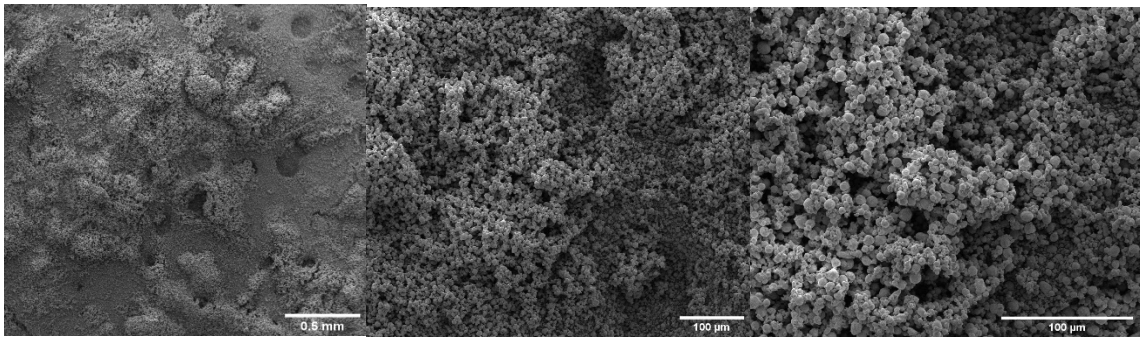

Figure 18. Area one. Copper (Cu-110) powder size at 1–5-micron mesh. Left 100x magnification; middle 500x magnification; right 1000x magnification

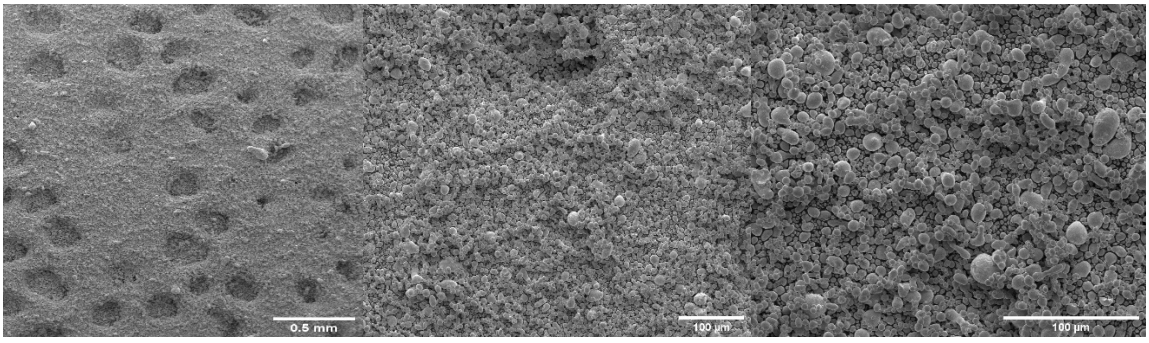

Figure 19. Area one. Tin (Sn-102) powder size at -325 mesh. Left 100x magnification; middle 500x magnification; right 1000x magnification

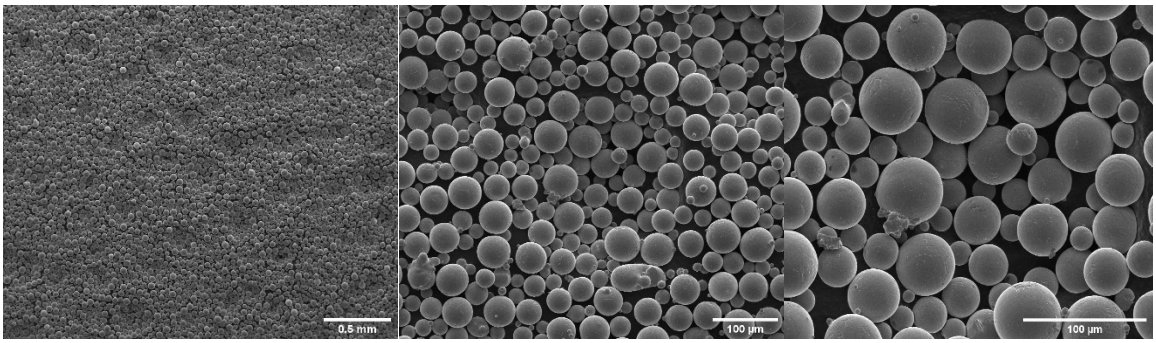

Figure 20. Area one. Titanium (Ti-64) powder. Left 100x magnification; middle 500x magnification; right 1000x magnification

B. PARTICLE SIZE MEASUREMENT

Three batches were conducted for each of the two powders, as seen in Table 8 and Table 9, the Canberra software provided mean size and standard deviation for four different frames of reference. From [27] and [28] the refractive index was found to be 0.23883 for copper and 2.15349 for titanium.

Table 8. Titanium powder mean size and standard deviation for different frame of reference.

	Batch 1		Batch 2		Batch 3	
Frame of Reference	Mean Size (µm)	Standard deviation (µm)	Mean Size (µm)	Standard deviation (µm)	Mean Size (µm)	Standard deviation (µm)
Area	36.62732	8.9094	36.07985	8.8126	35.65141	8.7084
Length	34.64404	8.1185	34.07858	8.1206	33.68525	8.0109
Numbers	32.88102	7.6138	32.20365	7.6078	31.85349	7.4897
Volume	38.88993	10.0147	38.30669	9.7989	37.84826	9.6974

Table 9. Copper powder mean size and standard deviation for different frame of reference.

Frame of Reference	Batch 1		Batch 2		Batch 3	
	Mean Size (μm)	Standard deviation (μm)	Mean Size (μm)	Standard deviation (μm)	Mean Size (μm)	Standard deviation (μm)
Area	5.57312	1.9028	4.85006	2.0871	5.30448	98.1987
Length	4.94888	1.7354	3.98188	1.8377	0.31106	0.0772
Numbers	4.36200	1.5765	3.19813	1.5681	0.29401	0.0708
Volume	6.23873	2.0967	5.79220	2.4016	1482.345	812.7048

As seen in Table 8, the titanium powder size is consistent across all three samples for each frame of reference. However, as seen in Table 9, the copper powder size is consistent in sample batches one and two, where batch three was inconsistent. Copper powder batches one and two are consistent with what was expected. As the manufacturer of the powder stated, a size range of 1–5-micron, the study considers batch three an error.

C. POLYMER SELECTION

The time of curing for the polymer candidates was found to be hours for the two-part epoxy, weeks for the UV formulation, and months for the Mowital B 30HH polyvinyl. Mowital B 30HH was determined to be incapable of supporting higher weight fractions, as seen in Table 10, which are needed to support the metal composite. This caused the study to downselect the use of Mowital B 30HH polymer.

Table 10. Mowital B 30HH weight fraction data.

Weight of Mowital B 30HH Wanted (g)	Weight of Mowital B 30HH Actual (g)	Weight of Ethanol Wanted (g)	Weight of Ethanol Actual (g)	Mowital Weight Fraction Wanted (%)	Mowital Weight Fraction Actual (%)	Solids Visible after Mixture
1	1.0004	4	4.0064	20	19.98	No
1.5	1.5068	3.5	3.5077	30	33.45	No
2	2.0043	3	2.9985	40	40.06	Yes
2.5	2.5023	2.5	2.4986	50	50.04	Yes
3	3.0084	2	2.0038	60	60.02	Yes
4	4.0083	1	1.0045	80	79.96	Yes

In addition, after curing it was recorded that the sample for 607105RCL13 UV Formulation polymer would read an open circuit condition for resistance. This is most likely due to the polymer's expansion, which would cause increased distance between individual particles. The study downselected the use of UV polymer. The study found the two-part epoxy would maintain resistance reads before and after curing, which led to the use of only the two-part epoxy in the antenna build.

D. ELECTRICAL MEASUREMENT OF THE METAL POLYMERS

The open circuit readings on the copper samples were unexpected and need to be examined in the future. Initial copper traces were found to be conductive in the initial trials. The Ti-64 composite conductivity layer was found to be less than 0.16 mm and that the sample was above the critical threshold, as described by percolation theory, at 70% volume fraction. This is consistent with data recorded in the experiment where the conductivity layer was measured and the upper boundary was recorded at 0.16mm.

E. VOLUME FRACTION CONVERSION

In addition, from [29] density for the metal composite polymer can be found by

$$\rho = f * \rho_f + (1 - f) * \rho_m \quad (1)$$

where ρ_f is the density of the metal filler and ρ_m is the density of the matrix [29]. f is the volume fraction of the filler [29]. Plugging in 4.43g/cm^3 for ρ_f from [30] and 1.15g/cm^3 for ρ_m from [31] with a volume fraction of 70%.

$$\rho = .7 * 4.43 g/cm^3 + (1 - .7) * 1.15 g/cm^3 = 3.446 g/cm^3 \quad (2)$$

Next, the volume fraction can be converted to a mass fraction with the equation from [29] by

$$f_w = \frac{f * \rho_f}{f * \rho_f + (1 - f)\rho_m} \quad (3)$$

where f_w is the mass fraction [29]. Using a 70% fraction by volume for the Ti-64 metal filler.

$$f_w = \frac{.7*4.43g/cm^3}{.7*4.43g/cm^3+(1-.7)1.15g/cm^3} = 0.89988 \approx 0.9 \quad (4)$$

A 0.9 mass fraction is 90% by weight for the Ti-64 metal powder filler in the composite polymer.

F. HDTV ANTENNA TESTING

As seen by the results of the antenna testing, high volume fractions of Ti-64 and the use of low cost PLA filament allowed conductive properties to develop. The AM process experienced difficulty in physically printing the designs; however, the AM process successfully printed complex designs.

The HDTV antennas the Ti-64 antenna identified 1 analog channel and 10 digital channels with an average signal strength of 58%, as seen in Figure 21, whereas the black PLA antenna identified zero analog channels and 20 digital channels with a signal strength of 55%, as seen in Figure 22. The black PLA antenna was a 30% size reduction, in order to print with the black PLA, due to the material not being available on the Ultimaker S5 Pro 3D printer. The black PLA with the reduced size found more digital channels than the Ti-64 composite material. Both antennas were in the 50% signal strength range. This clearly indicates the application of Ti-64 composite or black PLA would be more cost efficient than the production of a standard HDTV antennas.

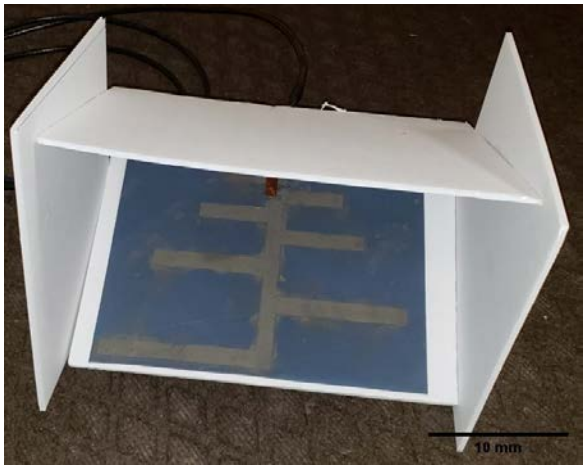

Figure 21. Ti-64 composite HDTV antenna

Figure 22. Black PLA HDTV antenna

G. WI-FI ANTENNA TESTING

The Wi-Fi antennas of the black PLA and the Ti-64 composite were not as effective as the original Tentsky antenna, but were more effective than only wires. The Tentsky repeater has an internal antenna and the wire is able to remove the effects of length when measuring the signal with a standard total wire length of 38.5 mm. The black PLA had a range between both antennas from -36dB to -54dB, as seen in Figures 23 and 25. On the other hand, the Ti-64 composite antennas had a range of -41dB to -49dB, as seen in Figure 24 and 26. This data identifies the Ti-64 composite are constant in the range of signal strength of a 8dB delta, were the black PLA had a delta of 18dB.

Figure 23. Black PLA Wi-Fi antenna

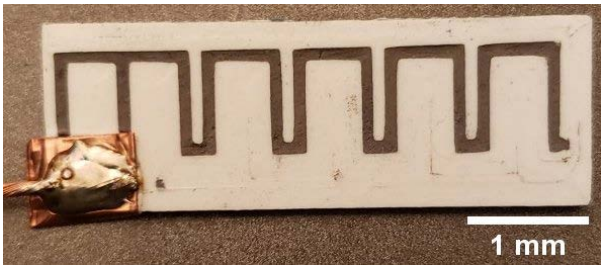

Figure 24. Ti-64 composite Linksys antenna

Figure 25. Black PLA Linksys antenna

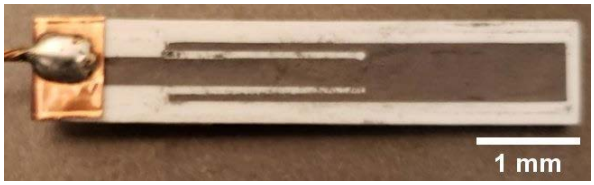

Figure 26. Ti-64 composite Wi-Fi antenna

However, the black PLA Linksys antenna had the strongest signal for the Wi-Fi antennas. Overall the minimum signal strength across all 3D printed antennas had an average increase over baseline of 9.25dB, confirming the viability of the black PLA material and the Ti-64 composite polymer material for applications in antennas.

IV. CONCLUSIONS

AM covers a wide array of building parts and tools, but limited attempts have been attempted to manufacture electrically conductive materials from 3D printing. This research investigated the AM of heterogeneous materials, including metal-polymer mixtures, under external fields and their potential applications. Specifically, the study analyzed how composition of the materials varied using different mass fractions of metal powders, such as copper and titanium mixed with polymer binders. During the extrusion and deposition of the materials, external fields were applied using a probe connected to a power supply that traversed the printed material. The path of the probe followed simple geometric shapes to generate conductive paths with identical shapes. The study optimized the process and downselected to one polymer and one metal. Two-part epoxy and titanium (Ti-64) were selected to build complex antenna shapes from a 3D printed mold. The results of this research confirmed the application of Ti-64 composite polymer as a viable low cost option for antenna application in HDTV signal range and 2.4GHz Wi-Fi signal range. In addition, this study helped to comprehend and improve the use of AM of metal-based conductive materials and their applicability to ship board uses.

THIS PAGE INTENTIONALLY LEFT BLANK

V. FUTURE WORK

The future work of the study will need to print Ti-64 and the two-part epoxy at 70% by volume test antennas in the 2.4 GHz, 5 GHz, and other ranges using a 3D printer. Once those antennas are printed, signal strength tests and thermal property tests will need to be conducted on the antennas. Next, the antennas will need to be corrosion tested in accordance with corrosion standards and wear standards of ASTM B117-19, “Standard Practice for operating salt spray (Fog) Apparatus,” and G1-03(2017)e1, “Standard Practice for Preparing, Cleaning, and Evaluating Corrosion Test Specimens,” to replicate a marine environment [32]. The antennas would then need to be dissected for examination. Afterwards, the study would need to examine the antennas under an optical microscope and SEM to identify structure failures or defects. In addition, the study would need to refine manufacturing techniques and expand the material selection into new metals and epoxies. Then, the study would need to incorporate antennas embedded into load bearing structures and evaluate the mechanical properties of the structures. Last, the future work of the study would need to continue to expand the understanding of electrically conductive 3D materials and applied fields on materials to improve properties. Thus, the study would need to continue to improve AM processes and techniques.

THIS PAGE INTENTIONALLY LEFT BLANK

APPENDIX. SEM MICROGRAPHS FOR AREA 2 AND AREA 3 OF METAL POWDERS.

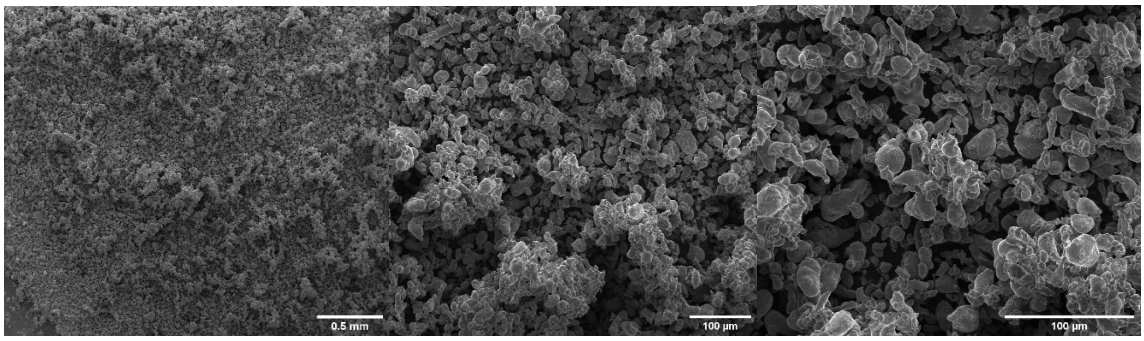

Figure 27. Area two. Aluminum (Al-101) powder size at -325 mesh. Left 100x magnification; middle 500x magnification; right 1000x magnification

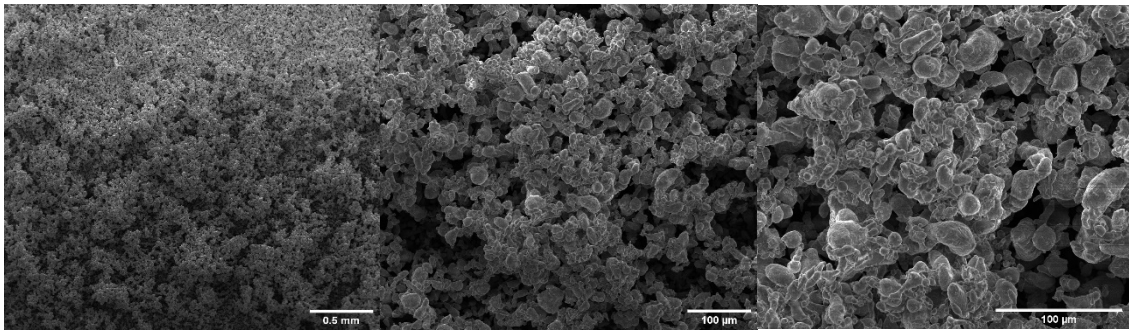

Figure 28. Area three. Aluminum (Al-101) powder size at -325 mesh. Left 100x magnification; middle 500x magnification; right 1000x magnification

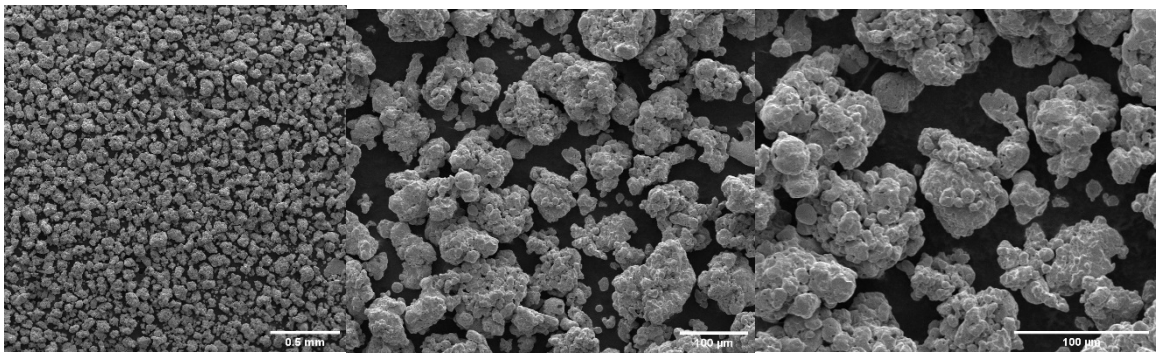

Figure 29. Area two. Copper (Cu-115) powder size at -100 mesh. Left 100x magnification; middle 500x magnification; right 1000x magnification

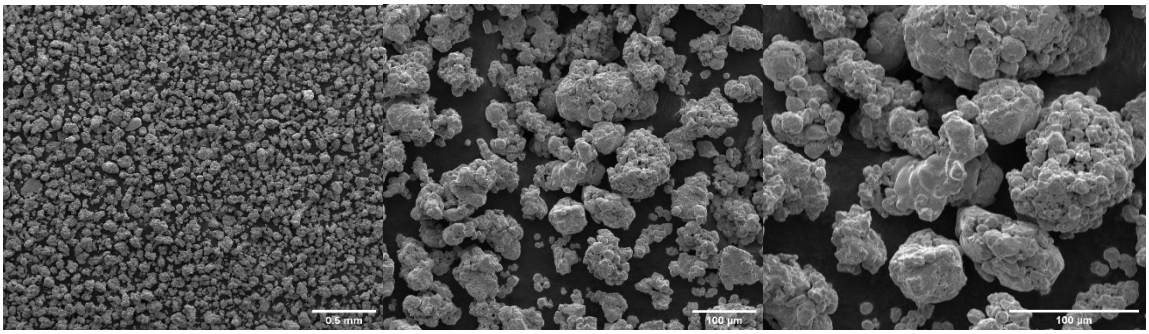

Figure 30. Area three. Copper (Cu-115) powder size at -100 mesh. Left 100x magnification; middle 500x magnification; right 1000x magnification

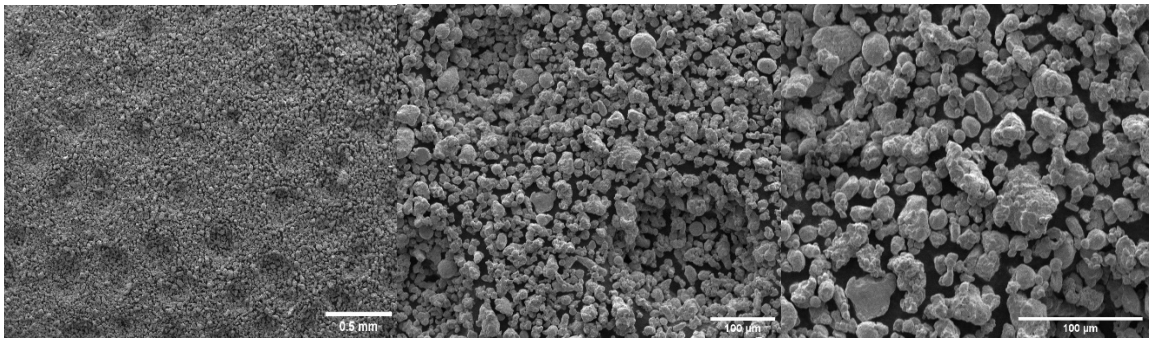

Figure 31. Area two. Copper (Cu-112) powder size at -325 mesh. Left 100x magnification; middle 500x magnification; right 1000x magnification

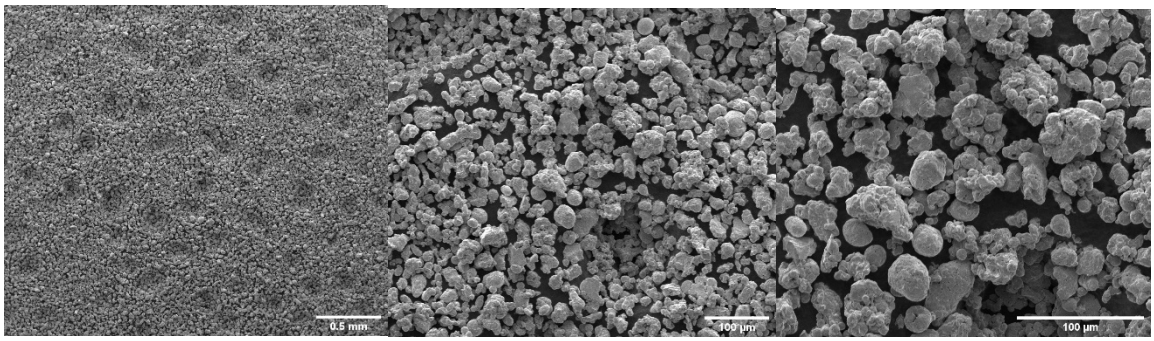

Figure 32. Area three. Copper (Cu-112) powder size at -325 mesh. Left 100x magnification; middle 500x magnification; right 1000x magnification

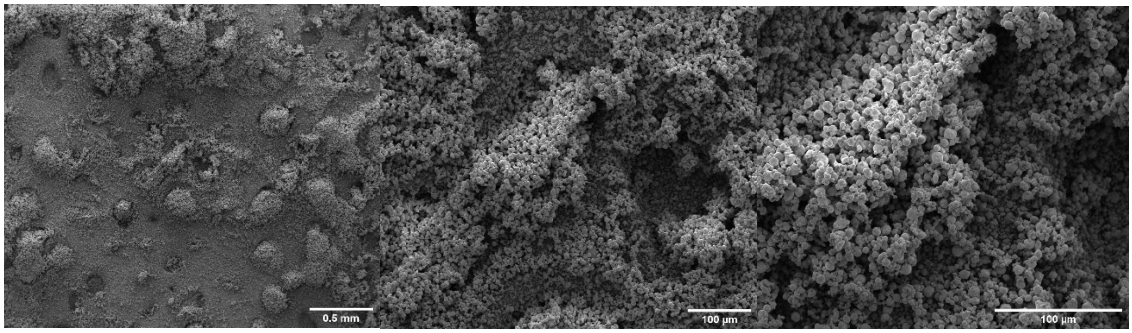

Figure 33. Area two. Copper (Cu-110) powder size at 1–5-micron mesh. Left 100x magnification; middle 500x magnification; right 1000x magnification

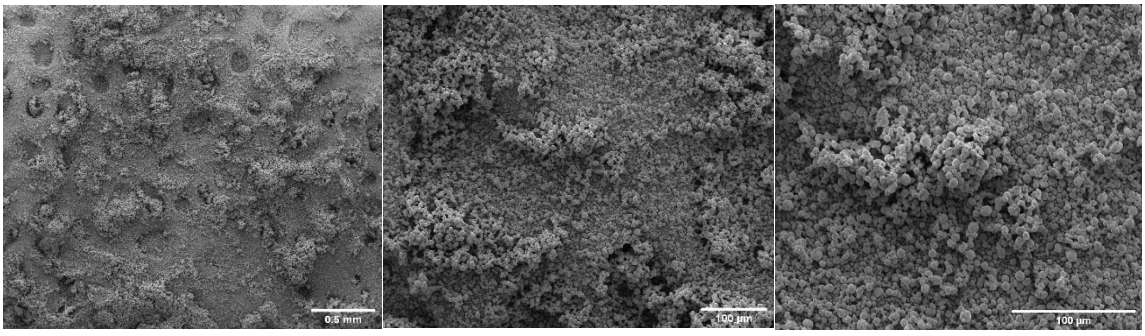

Figure 34. Area three. Copper (Cu-110) powder size at 1–5-micron mesh. Left 100x magnification; middle 500x magnification; right 1000x magnification

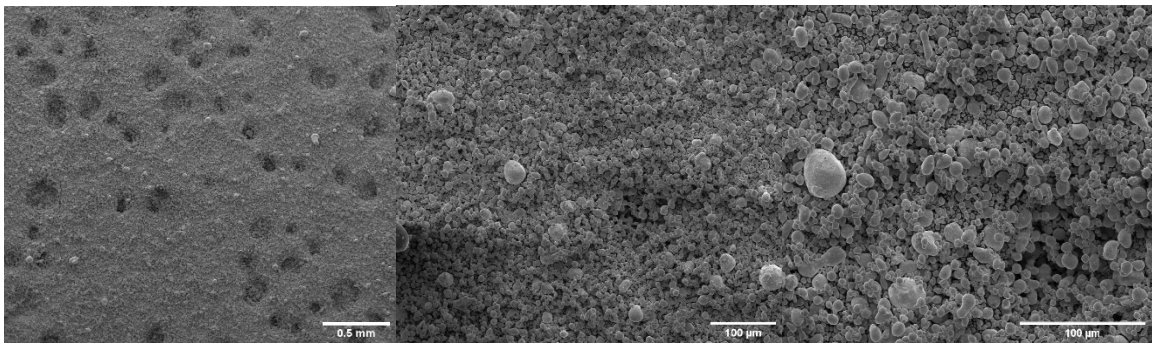

Figure 35. Area two. Tin (Sn-102) powder size at -325 mesh. Left 100x magnification; middle 500x magnification; right 1000x magnification

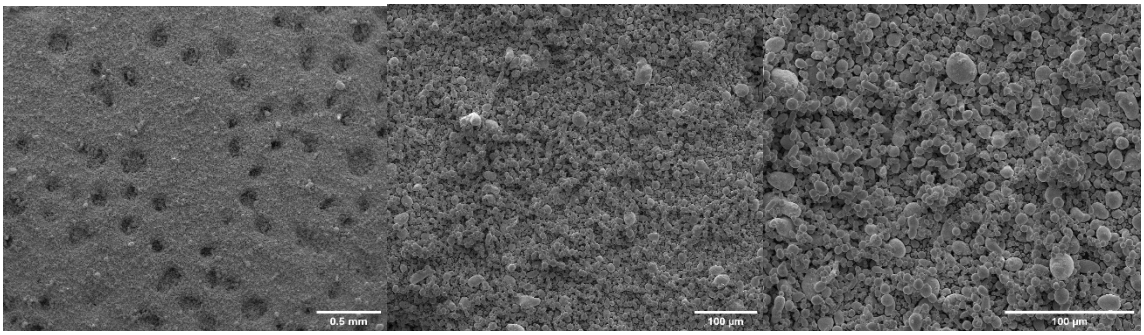

Figure 36. Area three. Tin (Sn-102) powder size at -325 mesh. Left 100x magnification; middle 500x magnification; right 1000x magnification

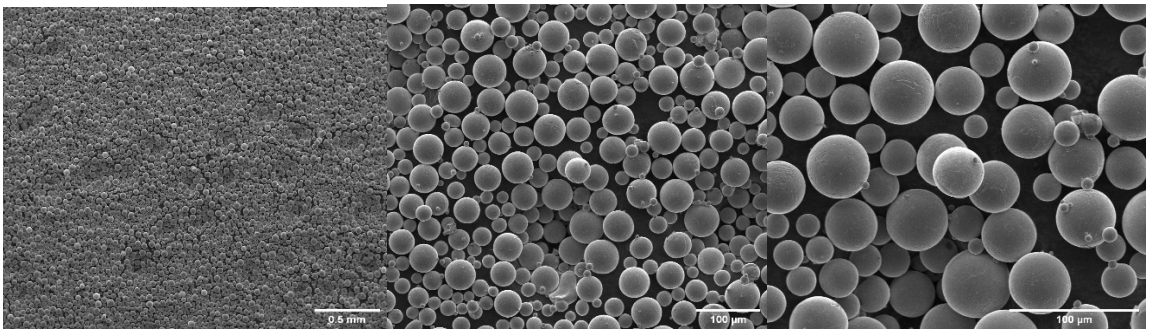

Figure 37. Area two. Titanium (Ti-64) powder. Left 100x magnification; middle 500x magnification; right 1000x magnification

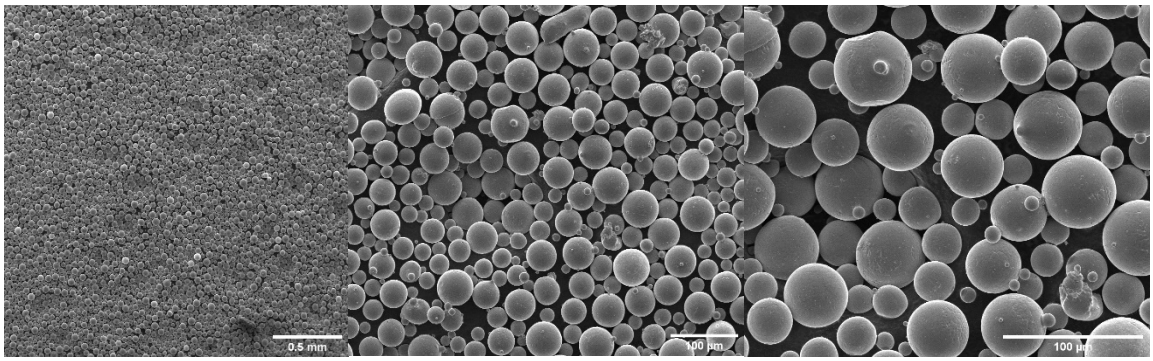

Figure 38. Area three. Titanium (Ti-64) powder. Left 100x magnification; middle 500x magnification; right 1000x magnification

THIS PAGE INTENTIONALLY LEFT BLANK

LIST OF REFERENCES

[1] P. Kocovic, “History of additive manufacturing,” in *3D printing and its impact on the production of fully functional components: emerging research and opportunities*, Hershey, PA: IGI Global, 2017, pp. 1–24.

[2] P. J. Springer, E. Alsuhibani, G. Sterley, J. Fallat and D. Bell, “The future of additive manufacturing in the U.S. military,” Air Command and Staff College Air University, 17 March 2017. [Online]. Available: https://apps.dtic.mil/dtic/tr/fulltext/u2/1042079.pdf

[3] T. J. Garino, “Electrical behavior of oxidized metal powders during and after compaction,” *Journal of Materials Research,* vol. 17, no. 10, pp. 2691–2697, Oct 2002.

[4] J. M. Montes, F. G. Cuevas and J. Cintas, “Electrical resistivity of metal powder aggregates,” *Metallurgical and Materials Transactions B,* vol. 38B, pp. 957–964, December 2007.

[5] J. M. Montes, F. G. Cuevas, J. Cintas and J. M. Gallardo, “Electrical conductivity of metal powder aggregates and sintered compacts,” *J Mater Sci,* vol. 51, pp. 822–835, 2016.

[6] M. P. Samuel and P. K. Philip, “Properties of compacted, pre-sintered and fully sintered electrodes produced by powder metallurgy for electrical discharge machining,” *Indian Journal of Engineering & Materials Sciences,* vol. 3, pp. 229–233, December 1996.

[7] K.-J. Euler, “The conductivity of compressed powders. A review,” *Journal of Power Sources,* vol. 3, pp. 117–136, 1978.

[8] M. A. Cruz, S. Ye, M. J. Kim, C. Reyes, F. Yang, P. F. Flowers and B. J. Wiley, “Multigram synthesis of Cu-Ag core-shell nanowires enables the production of a highly conductive polymer filament for 3D printing electronics,” *Particle & Particle Systems Characterization,* vol. 35, no. 1700385, pp. 1–10, 25 January 2018.

[9] F. F. T. de Araujo and H. M. Rosenberg, “Switching behaviour and DC electrical conductivity of epoxy-resin / metal-powder composites,” *Journal of Physics D: Applied Physics,* vol. 9, pp. 1025–1030, 1976.

[10] H. Nishikawa, S. Mikami, K. Miyake, A. Aoki and T. Takemoto, “Effects of silver coating covered with copper filler on electrical resistivity of electrically conductive adhesives,” *Materials Transactions,* vol. 51, no. 10, pp. 1785–1789, 2010.

[11] Y. Wang, C. Zhu, R. Pfattner, H. Yan, L. Jin, S. Chen, F. Molina-Lopez, F. Lissel, J. Liu, N. I. Rabiah, Z. Chen, J. W. Chung, C. Linder, M. F. Toney, B. Murmann and Z. Bao, “A highly stretchable, transparent, and conductive polymer,” *Science Advances Research Article Applied Sciences and Engineering,* vol. 3, no. e1602076, pp. 1–10, 10 March 2017.

[12] Y. Ebihara, N. Kunikyo, M. Kanda, R. Ohyama and Y. Nishi, “Electrical conductivity of Cu-powder dispersed PMMA composites prepared by solution-cast,” *The Japan Institute of Metals,* vol. 74, no. 11, pp. 712–717, 2010.

[13] C. Pierre, R. Deltour, J. A. A. J. Perenboom and P. J. M. Van Bentum, “Electrical-conduction mechanisms in polymer-copper-particle composites,” *Physical Review B,* vol. 42, no. 6, pp. 3380–3394, 15 August 1990.

[14] A. M. Lyons, “Electrically conductive adhesives: Effect of particle composition and size distribution,” *Polymer Engineering and Science,* vol. 31, no. 6, pp. 445–450, March 1991.

[15] R. R. Singh and R. W. Roberts, “Electrical resistivity behavior of solution-cast metal-filled composites,” *Polymer Composites,* vol. 6, no. 1, pp. 58–62, January 1985.

[16] N. N. Rozik, J. N. Asaad, S. H. Mansour and E. Gomaa, “Effect of aluminum and aluminum/nickel hybrid fillers on the properties of epoxy composites,” *Materials: Design and Applications,* vol. 230, no. 2, pp. 550–557, 2016.

[17] N. Boumedienne, Y. Faska, A. Maaroufi, G. Pinto, L. Vicente and R. Benavente, “Thermo-structural analysis and electrical conductivity behavior of epoxy / metals composites,” *Journal of Physics and Chemistry of Solids,* vol. 104, pp. 185–191, 18 January 2017.

[18] M. R. Nobile, L. Nicodemo, L. Nicolais, L. Egiziano, G. Lupo and V. Tucci, “The effect of the applied field on the electrical properties of metal polymer composites,” *Polymer Composites,* vol. 9, no. 2, pp. 139–143, April 1988.

[19] G. M. Tsangaris and M. C. Kazilas, “Conductivity and percolation in epoxy resin/conductive filler composites,” *Materials Science and Technology,* vol. 18, pp. 226–230, February 2002.

[20] S. H. Kwan, F. G. Shin and W. L. Tsui, “Direct current electrical conductivity of silver-thermosetting polyester composites,” *Journal of Materials Science,* vol. 15, pp. 2978 - 2984, 1980.

[21] V. R. Manikam, K. A. Razak and K. Y. Cheong, “Sintering of silver-aluminum nanopaste with varying aluminum weight percent for use as a high-temperature die-attach material,” *IEEE Transactions on Components, Packaging and Manufacturing Technology,* vol. 2, no. 12, pp. 1940–1948, December 2012.

[22] S. M. Musameh, M. K. Abdelazeez, M. S. Ahmad, A. M. Zihlif, M. Malinconico, E. Martuscelli and G. Ragosta, “Some electrical properties of aluminum-epoxy composite,” *Materials Science and Engineerring,* vol. B10, pp. 29–33, 1991.

[23] Eddy Current Technology Incorporated, “Conductivity of metals sorted by resistivity,” 14 November 2013. [Online]. Available: http://eddy-current.com/conductivity-of-metals-sorted-by-resistivity/.

[24] Brostown Technology, “Brostown 120Pcs 1/2” industrial liquid dispenser needle adhesive glue dispensing blunt tip luer lock,” [Online]. Available: https://www.amazon.com/Brostown-Industrial-Dispenser-Adhesive-Dispensing/dp/B077NZ9RPD. [Accessed 1 November 2020].

[25] Kipkay, “$5 DIY HDTV antenna! Get free TV!,” Kipkay Videos, LLC., 2019. [Online]. Available: https://www.youtube.com/watch?v=X_OhW02DmUs.

[26] D. Das, “How to design a PCB Antenna for 2.4GHz,” CircuitDigest, 27 May 2020. [Online]. Available: https://circuitdigest.com/article/how-to-design-a-pcb-antenna-for-24ghz.

[27] KLA Corporation, “Refractive index of Cu, copper,” Filmetrics, 2020. [Online]. Available: https://www.filmetrics.com/refractive-index-database/Cu/Copper#:~:text=Copper%20is%20a%20chemical%20element,nm%20are%200.23883%20and%203.415658..

[28] KLA Corporation, “Refractive index of Ti, titanium,” Filmetrics, 2020. [Online]. Available: https://www.filmetrics.com/refractive-index-database/Ti/Titanium#:~:text=Titanium%20is%20a%20chemical%20element,nm%20are%202.15349%20and%202.923488..

[29] J. Pilling, “Density, weight and voulme fractions,” 2011. [Online]. Available: https://sites.google.com/site/compositematerialsdesign/home/weight-and-volume-fractions.

[30] ASM Aerospace Specification Metals Inc., “Titanium Ti-6Al-4V (Grade 5), Annealed,” [Online]. Available: http://asm.matweb.com/search/SpecificMaterial.asp?bassnum=MTP641. [Accessed 17 November 2020].

[31] Epoxies Inc., “20-3237 clear flexible epoxy,” [Online]. Available: https://www.epoxies.com/_resources/common/bulletins/20-3237R.pdf. [Accessed 17 November 2020].

[32] ASTM International, “Corrosion standards and wear standards,” [Online]. Available: https://www.astm.org/Standards/corrosion-and-wear-standards.html. [Accessed 14 October 2020].

[33] All Metals Fabrication, “Which metal best conducts electricity?,” All Metals Fabrication, 28 March 2016. [Online]. Available: https://www.allmetalsfab.com/metal-best-conducts-electricity/

THIS PAGE INTENTIONALLY LEFT BLANK

INITIAL DISTRIBUTION LIST

1. Defense Technical Information Center
   Ft. Belvoir, Virginia

2. Dudley Knox Library
   Naval Postgraduate School
   Monterey, California